

## Synthesis of tetrakis bromine terminated phthalocyanine and its methyl methacrylate polymers via ATRP

Tuba ÇAKIR ÇANAK<sup>1</sup> , Damla YEŞİLDAG<sup>2</sup> , Ilgın NAR<sup>1</sup> , Esin HAMURYUDAN<sup>1</sup> ,  
İbrahim Ersin SERHATLI<sup>1,\*</sup> 

<sup>1</sup>Department of Chemistry, Faculty of Science and Letters, İstanbul Technical University, İstanbul, Turkey

<sup>2</sup>Department of Polymer Science and Technology, Institute of Science and Technology, İstanbul Technical University, İstanbul, Turkey

Received: 20.11.2018

Accepted/Published Online: 26.03.2019

Final Version: 11.06.2019

**Abstract:** A phthalocyanine (Pc) initiator, tetrakis(2-bromopropoxyester)ethylthiophthalocyaninatozinc(II) (ZnPc-Br), was prepared and successfully applied to atom transfer radical polymerization (ATRP) of methyl methacrylate (MMA) for the first time. Bromine end groups of the synthesized Pc took part in the initiation of the MMA chain growth. Polymerization was demonstrated by monomodal molecular weight distribution of the synthesized polymers and their increasing molecular weight behavior with reaction time. UV-Vis absorption, fluorescence, and transmittance properties of the polymers were also examined. The results indicate that the ZnPc-Br-based initiator is potentially applicable in ATRP applied to MMA in order to obtain and develop functional acrylic materials.

**Key words:** Phthalocyanine, poly(methylmethacrylate), atom transfer radical polymerization

### 1. Introduction

Phthalocyanines (Pcs), which have been extensively utilized as dyes and pigments,<sup>1</sup> have a unique chemical make-up suitable for wide applications, including gas sensors,<sup>2</sup> photovoltaic devices,<sup>3</sup> liquid crystals,<sup>4,5</sup> molecular magnets,<sup>6</sup> nonlinear optics,<sup>7</sup> and photosensitizers for photodynamic cancer therapy.<sup>8,9</sup> Physicochemical properties of Pcs can be modified by introducing variations to the central metal atom or changing the type, number, or position of peripheral substituents.

Pcs have been incorporated into polymeric structures in order to obtain new materials with varying properties.<sup>10–20</sup> For the synthesis of new functional materials, a combination of controlled radical polymerization methods with Pcs is practical and convenient.<sup>21,22</sup>

There are three extensively used common controlled radical polymerization techniques, including atom transfer radical polymerization (ATRP),<sup>23,24</sup> reversible addition fragmentation chain transfer polymerization (RAFT),<sup>25</sup> and nitroxide mediated radical polymerization.<sup>26</sup> All of these methods allow us to check the molecular weight and narrow distributions by depressing the number of radical species active during polymerization. Using ATRP, Duan et al. synthesized an end-functionalized poly(*N*-isopropylacrylamide) (PNIPAM) with a nonsymmetrical Pc. The well-defined polymers obtained after combining Pcs and PNIPAM displayed photocatalytic activity that was verified with oxidative degradation of rhodamine B in aqueous solution.<sup>27</sup> Well-defined side-chain phthalonitrile and zinc Pc-containing polymers were synthesized via RAFT.<sup>28</sup> Other studies

\*Correspondence: serhatli@itu.edu.tr

have reported polymers containing a terminal Pc core. For example, Kimura et al. realized the synthesis of polyacrylate-containing amphiphilic PCs through controlled/living radical polymerization from a Pc-containing initiator and it showed self-assembly in the solution into fibrous aggregates.<sup>29</sup> In another study, Torres et al. described the synthesis of polymers, terminated with amphiphilic Pc, using ATRP of styrene from an initiator functionalized with Pc and studied its self-organization in solution.<sup>10</sup> The synthesis of Pc-bearing polystyrene and poly(*tert*-butyl acrylate), in which the Pc is either an end-group or serving as a macrocyclic core, was investigated using Huisgen 1,3-dipolar cycloaddition catalyzed by Cu(I) compound (commonly referred to as the click reaction) between nonsymmetrical Pcs and Pcs having symmetrical (terminal alkynyl) groups at the periphery and azide terminated polystyrene and poly(*tert*-butyl acrylate).<sup>30</sup>

Thekkatt et al. reported the synthesis and characterization study of a soluble and hydrophilic semiconductor, in which they used grafting-to of a nonsymmetrical copper Pc with azide functionality to a styrene backbone.<sup>31</sup> Recently, our group reported the synthesis of a new functional polystyrene polymer with a zinc Pc terminal that involved a click reaction between nonsymmetrical terminal-alkynyl-containing zinc Pc and azide-end functional polystyrene.<sup>32</sup>

Poor solubility and slippery  $\pi-\pi$  stacks restricted the applications of Pcs. Overcoming these limitations required several attempts.<sup>33,34</sup> Both symmetrical and nonsymmetrical Pcs, substituted with oligo ethylene glycol substituents, have been reported.<sup>35,36</sup> McKeown et al. synthesized water-soluble Pc-centered poly(ethyleneoxy) polymers prepared by the cyclotetramerization of phthalonitrile-containing oligo(ethyleneoxy) precursor compounds and investigated their properties.<sup>37,38</sup>

Synthesis of a star-shaped polytetrahydrofuran having a Pc core and their liquid crystalline properties were reported by Gursel et al.<sup>4</sup> Because of the complicated and time-consuming reaction and purification steps, it can be exhausting to synthesize star polymers with a Pc core using conventional methods. In another study, synthesis of a star-shaped Pc compound with four- or eight-length oligo(*p*-phenylenevinylene) side chains and their self-organization properties were described.<sup>39</sup> Recently, two studies were published on the synthesis of star-shaped polymers employing a metallophthalocyanine core as a tunable charge storage material for nonvolatile transistor memory devices via ATRP with styrene.<sup>24,40</sup> Here, we demonstrate the synthesis of symmetrical tetrakis (terminal bromine)-substituted Pc involved in ATRP reaction of MMA to yield star-like polymers, which, to the best of our knowledge, have never been reported. Introducing the terminal bromine groups to the four identical end sides of Pc actualized the controlled polymerization. The terminal bromine function on tetrakis(2-bromopropoxy)ethylthiophthalocyaninatozinc(II) allowed a facile polymerization of MMA through a Cu(I)-catalyzed ATRP reaction.

The target product, ZnPC-PMMA with a Pc core, has been described and characterized. Furthermore, electrochemical and spectrochemical properties of the obtained star-like Pc-containing MMA polymers, including electronic absorption, fluorescence, transmittance, and thermal properties, were investigated.

## 2. Results and discussion

### 2.1. Synthesis of ZnPc-Br

ZnPc-OH was functionalized to obtain a new initiator that was used for polymerization of methyl methacrylate (MMA). For this purpose, the ZnPc-OH core was esterified with 2-bromopropionyl bromide to obtain reactive bromine groups at the end. Figure 1 shows the synthesis of ZnPc-Br, which was used for the polymerization of MMA.

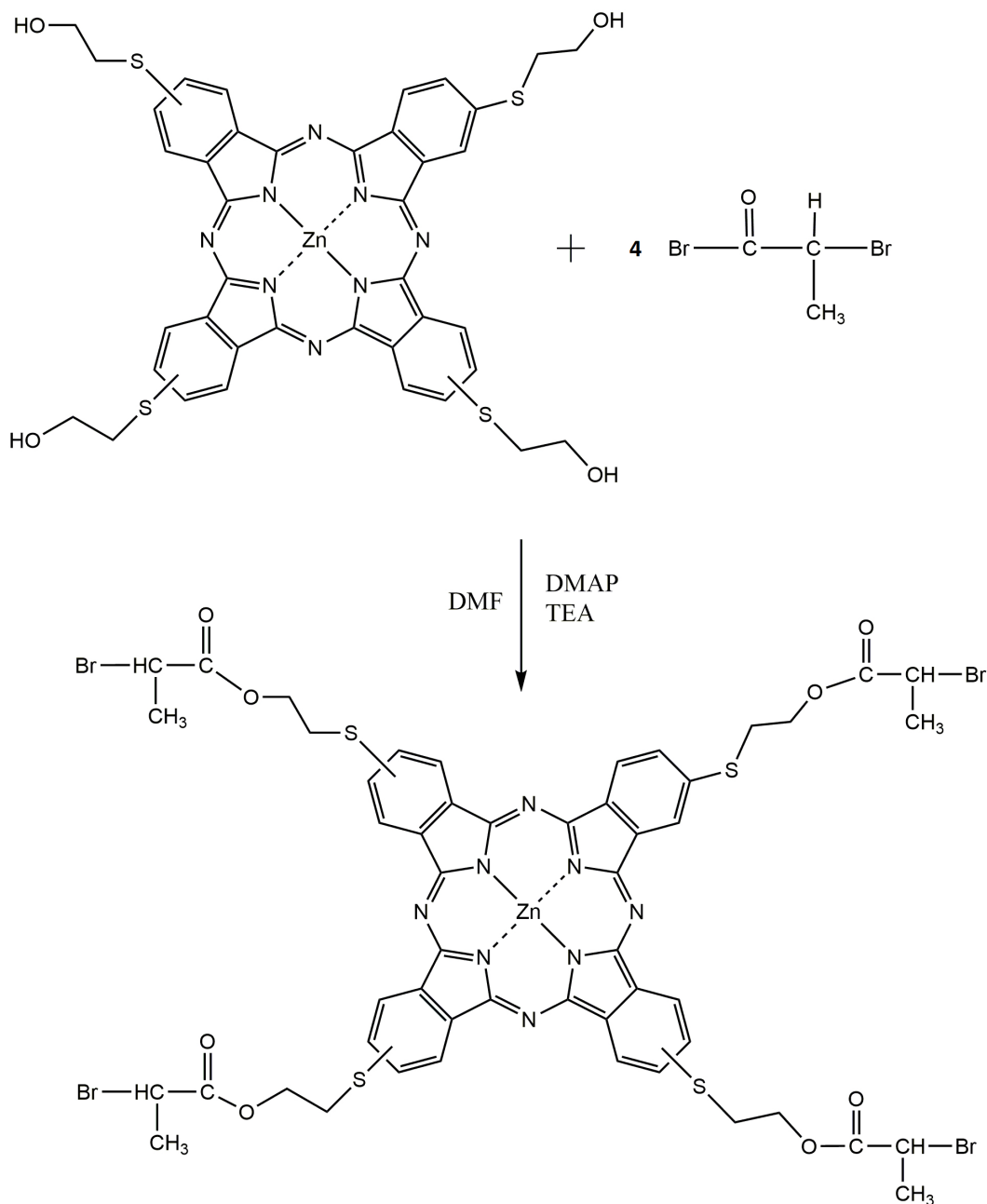


**Figure 1.** Synthesis of ZnPc-Br.

The spectrum of ZnPc-OH indicated eight *Ar*-H protons at 9.05 ppm, four *Ar*-H protons at 8.10 ppm, -OH protons at 5.25 ppm, -OCH<sub>2</sub> protons at 4.00 ppm, and -SCH<sub>2</sub> protons at 3.60 ppm.<sup>41</sup>

The <sup>1</sup>H NMR spectrum of ZnPc-Br was recorded in DMSO-*d*<sub>6</sub> and, as seen in the NMR spectrum of ZnPcBr in Figure 2, new peaks appeared at 4.71 ppm (quartet), 1.81 ppm (doublet), and 3.80 ppm (triplet) for -CH-Br, -CH<sub>3</sub>, and -OCH<sub>2</sub> protons, respectively.

There are four (-CH) “d” protons showing signals at 4.71 ppm (quartet), four (-ArH) “b” protons showing signals at 8.05 ppm, and eight (-ArH) “a” and “c” protons showing signals between 8.60 and 8.84 ppm as

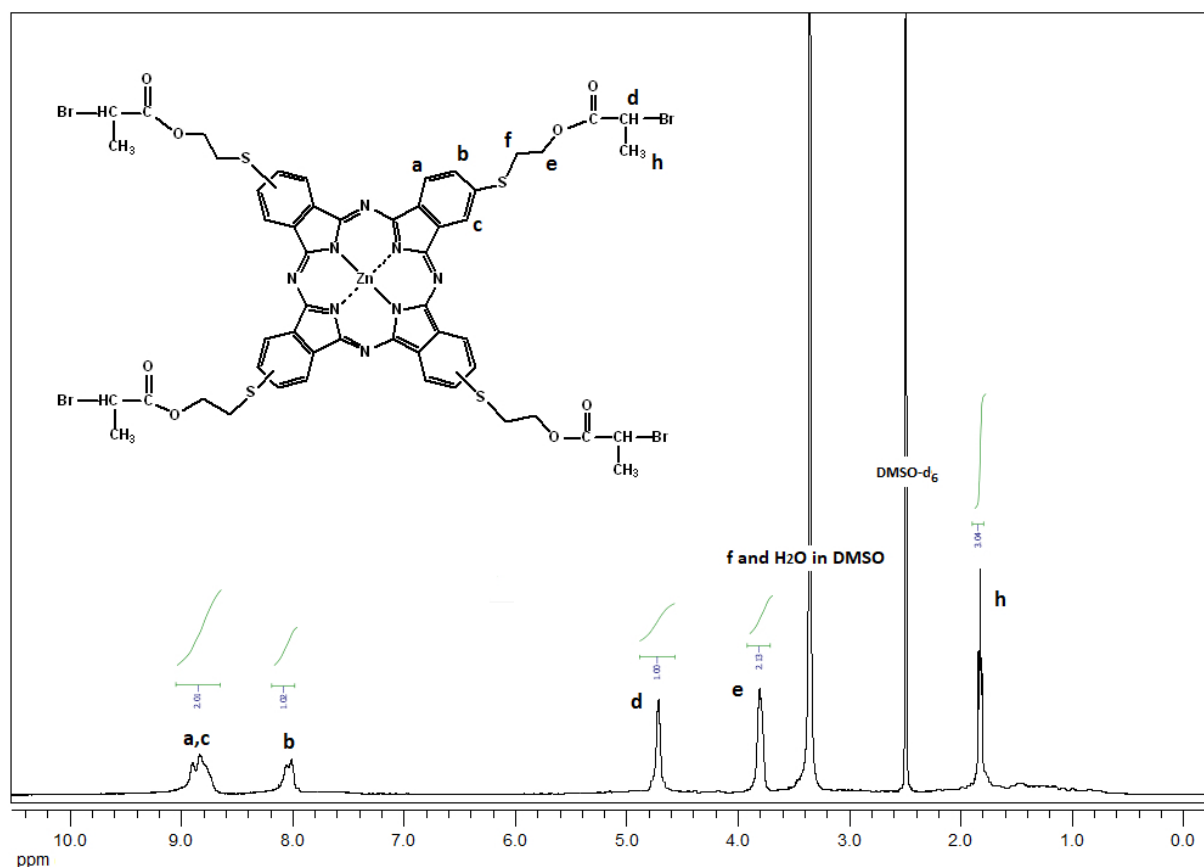


Figure 2.  $^1\text{H}$  NMR spectrum of ZnPc-Br in  $\text{DMSO-}d_6$ .

multiplets. Integration values of these three peaks were compared to each other and were 1.00, 1.02, and 2.01, respectively, meaning that all four arms of the Pc scaffold were functionalized with the groups including bromine. The peak for  $-\text{SCH}_2$  protons was not very clear because it overlapped with the peak of  $\text{H}_2\text{O}$  protons as an impurity in  $\text{DMSO-}d_6$ . In NMR for  $\text{DMSO-}d_6$  the intermolecular rate of exchange is slow enough that a peak due to HDO is usually also observed and it appears at 3.30 ppm in  $\text{DMSO-}d_6$ .

## 2.2. ATRP of methyl methacrylate

Figure 3 indicates that the ZnPc-Br initiator with bromine groups was employed to serve as an initiating entity of the ATRP of MMA for preparing four-armed polymers.

For controlled/living polymerization systems, it is a basic requirement to increase the monomer conversion with time. Moreover, as the conversion increases with time, polydispersities decrease during polymerizations.<sup>42–45</sup> As can be seen from Table 1, in our polymerization system, the results also showed the same behavior. However, we obtained broad molecular weight distributions (polydispersity index) and higher experimental  $M_n$  values (with gel permeation chromatography (GPC)) than those calculated. The polydispersity index values were between 1.71 and 1.36. Besides, when we increased the reaction time, the conversions of ZnPc-PMMA increased from 5.25% to 14.37%. The reason for this could be the low initiation efficiency of the initiator. For a good controlled ATRP, better correlating of the structures of the initiator with the monomer is necessary. More efficient initiation is provided when the monomer's chemical structure is similar to the initiator's.<sup>46</sup>

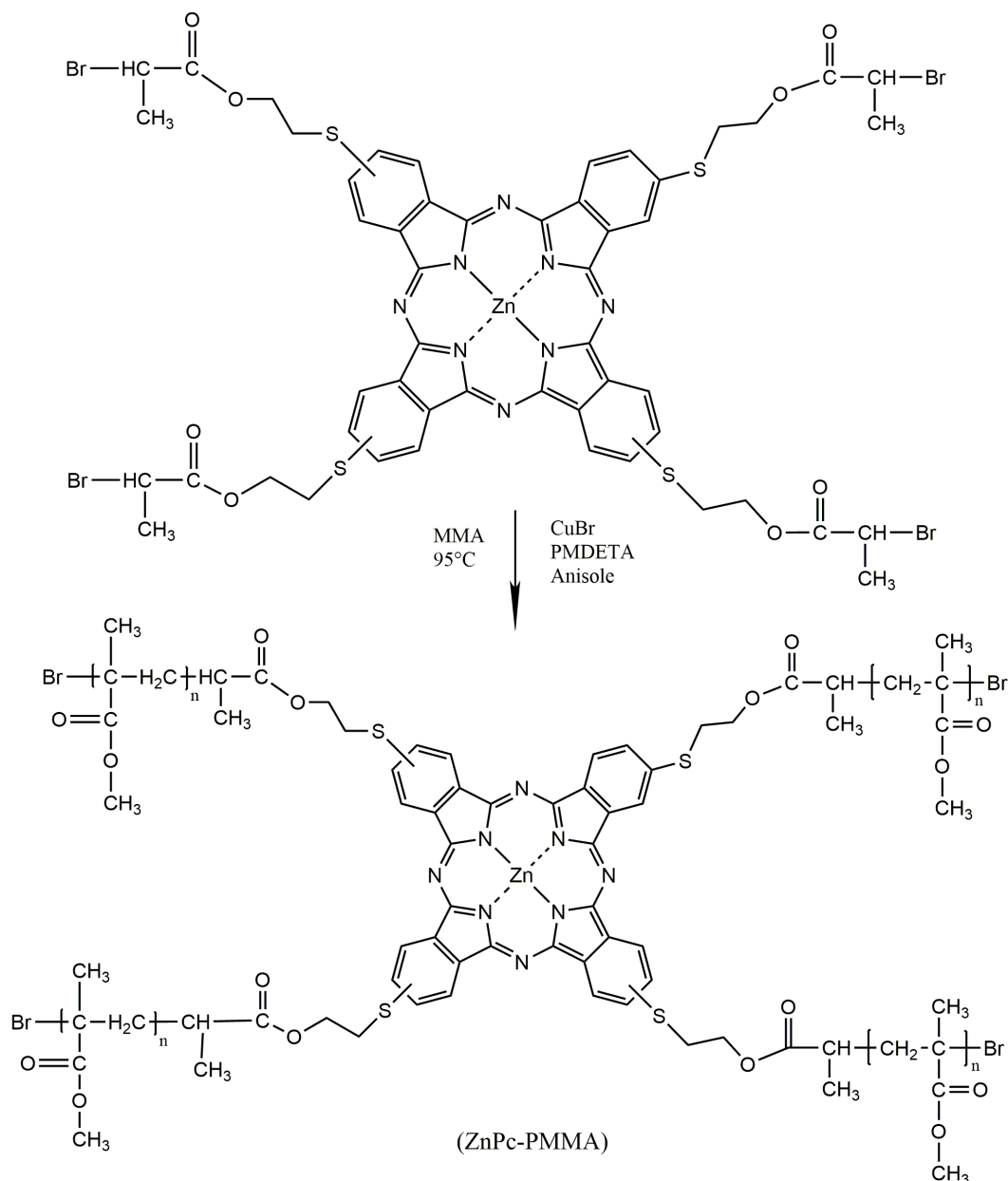


**Figure 3.** Synthesis of ZnPc-cored PMMAs using ZnPc-Br as an initiator.

The steric hindrance of ZnPc-Br also explains the uncontrolled behavior (it means that polydispersity indexes are a little higher compared to normal ATRP systems, not totally uncontrolled). It could be difficult to add a new monomer, so the chains preferred termination with the combination of two building chains, thereby resulting in high  $M_n$  and polydispersity index. Imperfections like termination, slow initiation, slow exchange, transfer, and their collective effects on polydispersities, kinetics, and molecular weight of living chain growth polymerization can be clarified by further research.<sup>47</sup>

The kinetic plots of polymerization of MMA are presented in Figure 4, in which  $[M]_o$  is the initial monomer concentration and  $[M]_t$  is the concentration of the monomer at time  $t$ . Even though it can be said that the initiator efficiency was low, the linearity of the semilogarithmic plot of  $\ln([M]_o/[M]_t)$  vs. time indicates

**Table 1.** Polymerization characteristics of ZnPc-PMMA.

Initiator	Run <sup>a</sup>	Time (h)	Conv. (%) <sup>b</sup>	$M_{n, th}$ <sup>c</sup> (g/mol)	$M_{n, exp}$ <sup>d</sup> (g/mol)	$M_w/M_n^d$
ZnPc-Br	ZnPc-PMMA4	6	5.22	11874	19937	1.71
ZnPc-Br	ZnPc-PMMA5	12	9.80	21045	37502	1.58
ZnPc-Br	ZnPc-PMMA6	24	12.75	26952	47217	1.55
ZnPc-Br	ZnPc-PMMA7	48	14.37	30196	50120	1.36

<sup>a</sup> Initial concentration ratios were  $[I]_o/[CuBr]_o/[PMDETA]_o/[M]_o = 1/7/14/2000$  in anisole at 95 °C.

<sup>b</sup> Determined gravimetrically.

<sup>c</sup> The theoretical number-average molecular weight.  $M_{n, th} = ([M]_o/[I]_o) \times (\text{conversion } \%) \times M_{monomer} + M_{initiator}$  ( $M_{monomer} = 100.12$  g/mol for MMA and  $M_{initiator}(\text{ZnPc-Br}) = 1422.24$  g/mol).

<sup>d</sup> Determination was performed by GPC analysis with PMMA standards.

that the polymerization was first-order with respect to the monomer and that the concentration of the growing radicals remained constant for 6, 12, and 24 h of polymerization times. However, after 24 h of reaction time, since termination occurs continuously, the concentration of the Cu(II) species increases and deviation from linearity was observed. For the ideal case with chain length-independent termination, persistent radical effect kinetics implies that the semilogarithmic plot of monomer conversion vs. time to the 2/3 exponent should be linear.<sup>48</sup> Nevertheless, a linear semilogarithmic plot is often observed. This may be due to an excess of the Cu(II) species present initially, a chain length-dependent termination rate coefficient, and heterogeneity of the reaction system due to limited solubility of the copper complexes. It is also possible that self-initiation may continuously produce radicals and compensate for termination.<sup>49</sup> Similarly, external orders with respect to the initiator and Cu(I) species may also be affected by the persistent radical effect.<sup>50</sup>

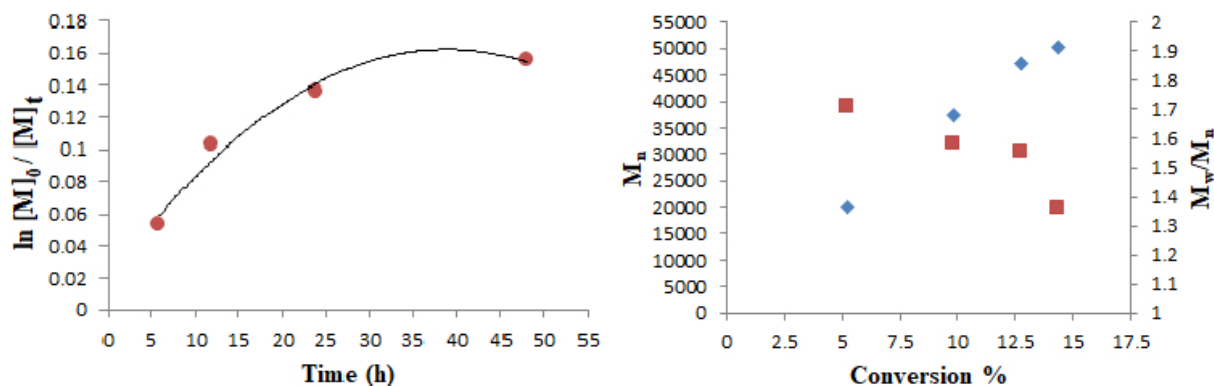


**Figure 4.** First-order kinetic plots for the polymerization of MMA using ZnPc-Br as an initiator and CuBr as catalyst in anisole at 95 °C.

As can be seen in Figure 4, the average molecular weights ( $M_n$ ) increased with conversion while the polydispersity indexes ( $M_w/M_n$ ) decreased. The calculations were  $[M]/[I]/[Cu]/[PMDETA] = 2000/1/7/14$  and  $[M_{MMA}]_o = 7.085$  M for polymerization with ZnPc-Br.

The GPC traces of the synthesized ZnPc-PMMA polymers obtained at different reaction times are shown in Figure 5. It can be seen that the molecular weights moved to a higher molecular weight region with monomodal distribution, showing that the MMA monomer converted to PMMA.

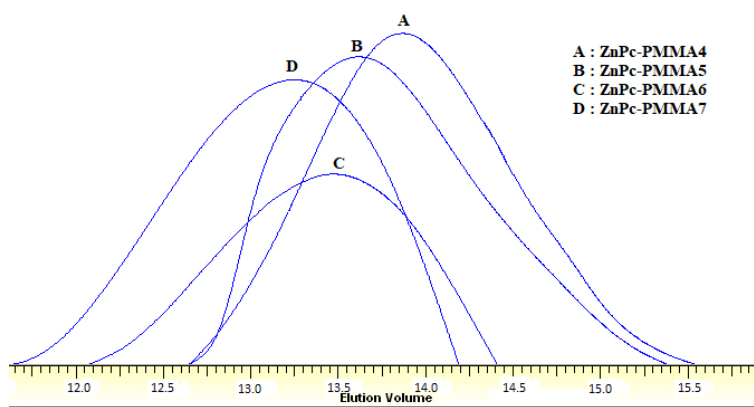


Figure 5. GPC traces of the ZnPc-PMMA polymers.

The FTIR spectra of the ZnPc-PMMA polymers, ZnPc-Br and ZnPc-OH, are presented in Figure 6. In the FTIR spectra of ZnPc-Br, the disappearance of the characteristic peak of the hydroxyl group around  $3280\text{ cm}^{-1}$  indicated that all the OH groups were brominated and the appearance of the C-Br band at  $677\text{ cm}^{-1}$  and C=O in the carboxyl group at  $1728\text{ cm}^{-1}$  confirmed that the targeted structure was synthesized successfully. Similar FTIR spectra are observed for all ZnPc-PMMA polymers. There is a band from  $1146\text{ cm}^{-1}$  to  $1269\text{ cm}^{-1}$  and it was attributed to the C-O-C stretching vibration.  $\alpha$ -Methyl group vibrations are seen at  $1386\text{ cm}^{-1}$  and  $750\text{ cm}^{-1}$ . Characteristic absorption vibrations of PMMA are seen at  $987\text{ cm}^{-1}$ ,  $1062\text{ cm}^{-1}$ , and  $841\text{ cm}^{-1}$ . The acrylate carboxyl group is shown at  $1726\text{ cm}^{-1}$ . The methyl group's bending vibration is shown at  $1435\text{ cm}^{-1}$ . The C-H stretching vibrations for  $-\text{CH}_3$  and  $-\text{CH}_2-$  groups are assigned to the two bands at  $2991\text{ cm}^{-1}$  and  $2950\text{ cm}^{-1}$ , respectively. It could be concluded, on the basis of the above discussion, that ZnPc-PMMA4 was indeed the prepared polymer.<sup>51</sup>

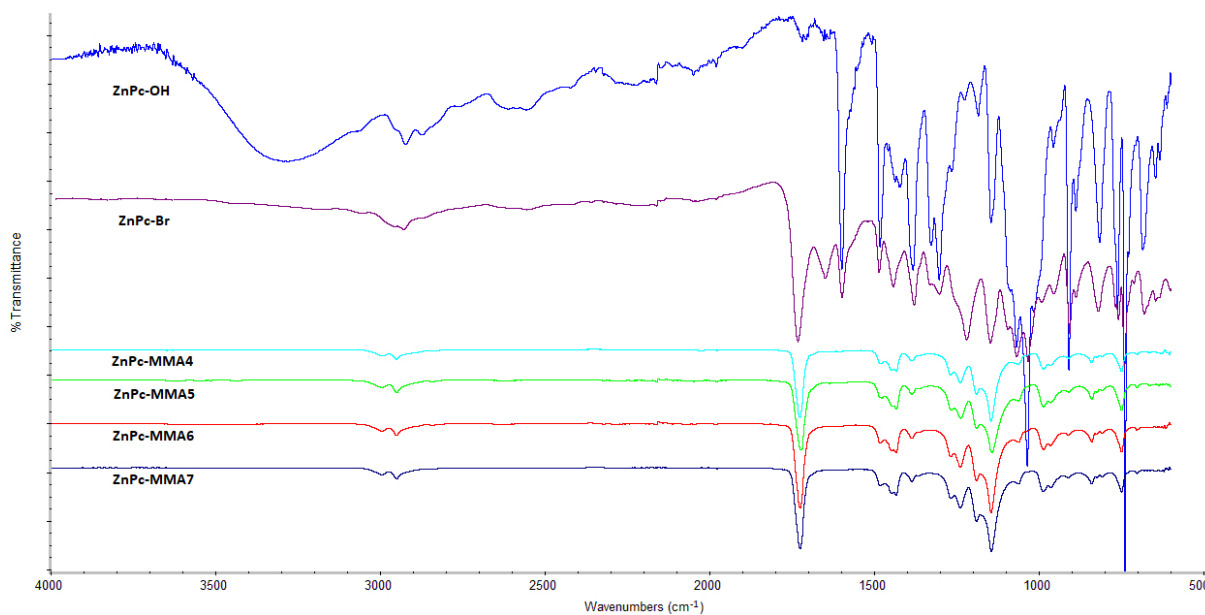


Figure 6. FTIR spectra of ZnPc-OH, ZnPc-Br, and ZnPc-PMMA polymers.

The  $^1\text{H}$  NMR spectrum of ZnPc-PMMA4 polymer was recorded in  $\text{CDCl}_3$  and is presented in Figure 7. The CH-Br signals were not observed in the spectrum of ZnPc-PMMA, indicating that bromine groups performed their work in the initiation of the PMMA chain growth. Figure 7 shows that the Ar-H protons of the Pc group had their chemical shifts at 9.4 ppm (multiplet), 8.2 ppm (multiplet), and 7.2 ppm (multiplet). The spectrum of the polymer clearly indicated the presence of  $-\text{SCH}_2$  at 3.8 ppm (multiplet) and  $-\text{OCH}_2$  at 4.5 ppm (multiplet) coming from the initiator.

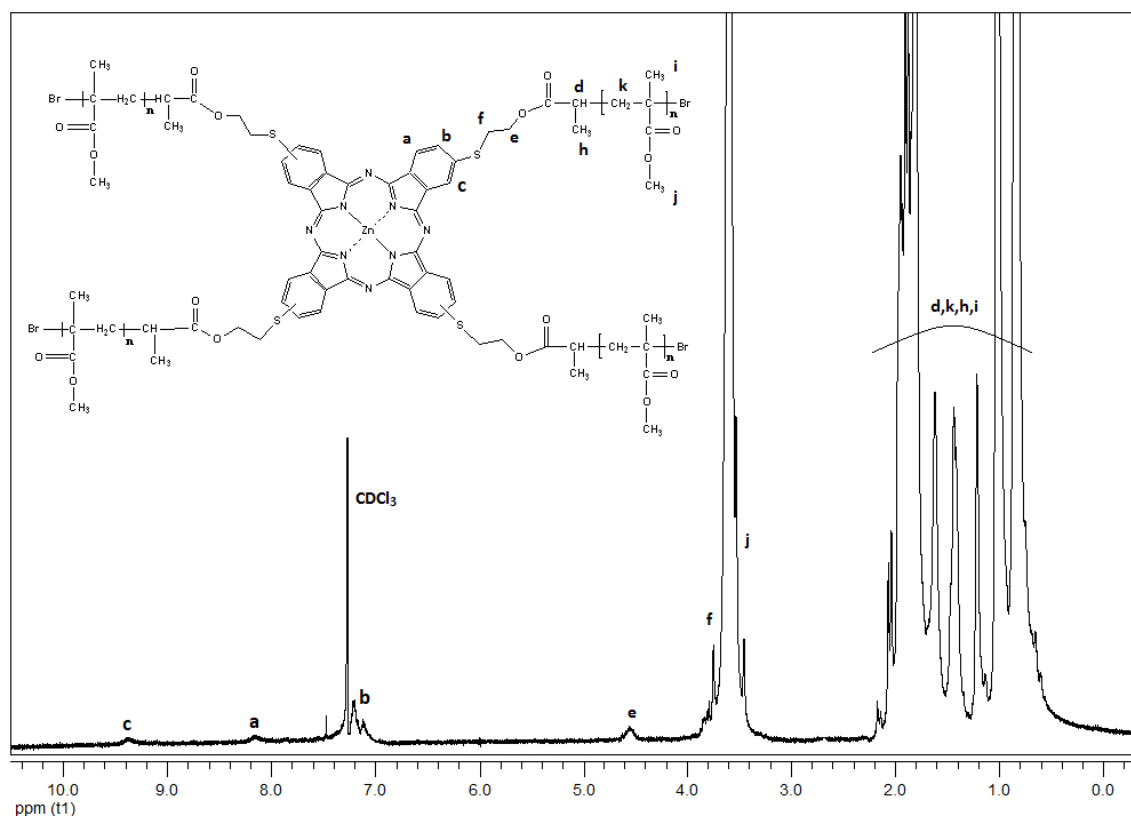


Figure 7.  $^1\text{H}$  NMR spectrum of ZnPc-PMMA4 polymer in  $\text{CDCl}_3$ .

The methylene protons of ZnPc-MMA and the initiator ZnPc-Br were indicated by the signals observed between 0.5 and 2.0 ppm. In addition, the peak at 3.6 ppm (multiplet) indicated the characteristic  $-\text{OCH}_3$  group of PMMA.

Unfortunately, the results of  $^1\text{H}$  NMR analysis of the ZnPc-MMA polymers make it hard to perform calculations of molecular weights via Pc core analysis, because the signal at 3.58 ppm from the  $-\text{OCH}_3$  in the MMA for ZnPc-MMA polymer was obscure and it interfered with the  $-\text{SCH}_2$  protons in the same region.

### 2.3. Electrochemical properties

Electrochemical studies were carried out to find the redox potentials of Pc compounds. Cyclic and square wave voltammograms of ZnPc-Br and ZnPc-PMMA4 are shown in Figure 8 and provided in Table 2.

Both compounds displayed two reduction and two oxidation waves vs. saturated calomel electrode (SCE). The basic electrochemical parameters of Pcs are in harmony with similar complexes observed in the literature.<sup>30,52–54</sup> Between ZnPc-Br and ZnPc-PMMA4 recorded in dimethyl formamide, the main electro-



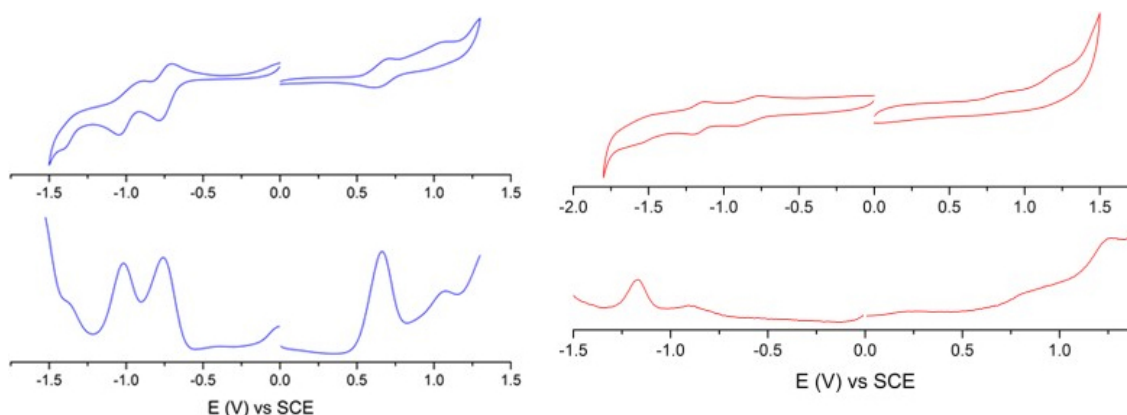


**Figure 8.** CV and SWV of ZnPc-Br (blue) and ZnPc-PMMA4 (red) in deaerated DMF using tetrabutylammonium perchlorate as the supporting electrolyte.

**Table 2.** Oxidation/reduction potentials of ZnPc-Br and ZnPc-PMMA4.

Sample	R <sub>1</sub> (V)	R <sub>2</sub> (V)	O <sub>1</sub> (V)	O <sub>2</sub> (V)
ZnPc-Br	-0.76	-1.01	0.66	1.07
ZnPc-PMMA4	-0.88	-1.17	0.85	1.25

chemical difference is the shift of reduction potentials of PMMA to the negative side and oxidation potential to the positive side when compared to ZnPc.

#### 2.4. Thermal behavior of ZnPc-PMMA

The polymers' thermal behaviors were investigated with differential scanning calorimetry (DSC) and thermogravimetric analysis (TGA). A heating rate of 10 °C/min was applied to DSC measurements. TGA under nitrogen at a heating rate of 20 °C/min was employed to measure the thermal stability. Table 3 summarizes the thermal analysis results.

**Table 3.** DSC and TGA results for ZnPc-PMMA polymers.

Sample	T <sub>g</sub> (°C)	T <sub>50%</sub> (°C) <sup>b</sup>	Residue at 500 °C (%)
ZnPc-PMMA4	116.5	400.1	6.1
ZnPc-PMMA5	121.0	393.5	3.7
ZnPc-PMMA6	129.7	394.1	4.8
ZnPc-PMMA7	129.8	392.9	1.3
STD PMMA <sup>a</sup>	120.0	391.6	2.0

<sup>a</sup> Molecular weight of pure PMMA is 30350 g/mol.

<sup>b</sup> T<sub>50%</sub> is the temperature value at which the sample is 50% decomposed.

The T<sub>g</sub> values of ZnPc-PMMA are in the range of 116–129 °C. These values are not significantly different from the T<sub>g</sub> values of standard PMMA as shown in Figure 9, but they are slightly higher.

It could be said that the macrocyclic compound that we used as an initiator could affect the T<sub>g</sub> by hindering the molecular motions of polymer chains sterically as the molecular weights of ZnPc-PMMA increase.

Degradation of the ZnPc-PMMA polymers as a function of temperature under nitrogen atmosphere is shown in Figure 10. When the polymer's molecular weight increases, the  $T_{50\%}$  temperature value, at which the sample is 50% decomposed, decreases. When the polymers' molecular weights increase, there will be fewer chain ends, which will cause smaller residue values, but still they do not have a linear relationship.

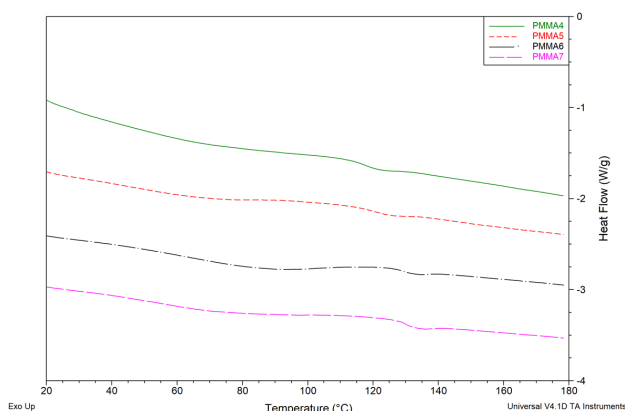


Figure 9. DSC thermograms of ZnPc-PMMA polymers.

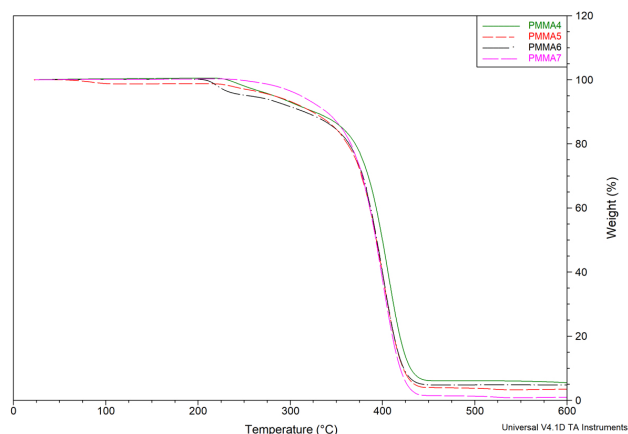


Figure 10. TGA thermograms of ZnPc-PMMA polymers.

## 2.5. Electronic absorption and fluorescence spectra

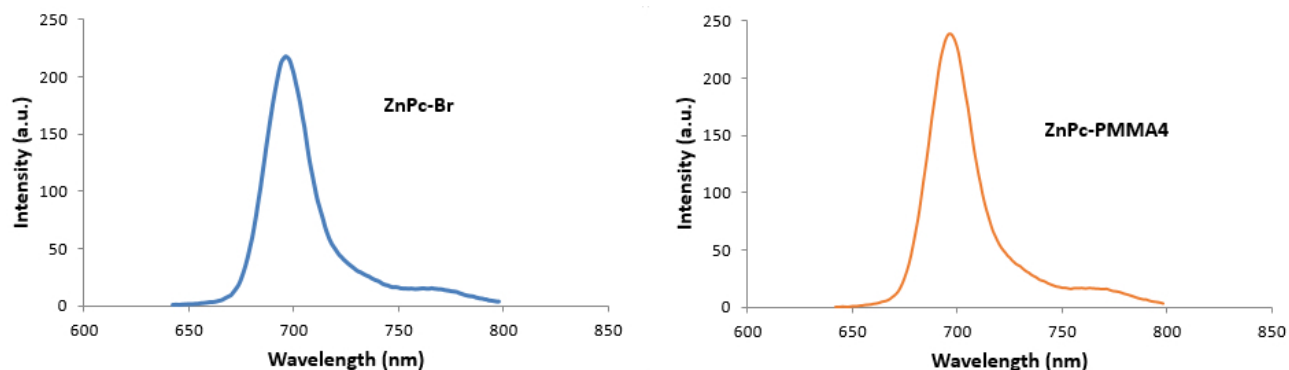
The Pcs present two strong absorption bands; one of them is the B band at about 300–400 nm and the other is the Q band at 600–750 nm in a typical electronic spectrum.<sup>5</sup> For ZnPc-Br, an intense Q band was observed at 687.5 nm and a B band was observed at 358 nm. Table 4 shows that the Q and B band maxima and all Q and B bands of ZnPc-PMMA are identical. Concentration values of ZnPc-Br, ZnPc-PMMA4, and ZnPc-PMMA5 are  $0.6 \times 10^{-5}$  M,  $1.7 \times 10^{-5}$  M, and  $3.1 \times 10^{-5}$  M, respectively.

Table 4. Electronic absorption spectral data for ZnPc-PMMA polymers.

Sample	Q band, $\lambda_{max}$ (nm)	B band, $\lambda_{max}$ (nm)
ZnPc-Br	687.5	358.0
ZnPc-PMMA4	688.0	357.0
ZnPc-PMMA5	688.0	357.0
ZnPc-PMMA6	688.0	359.5
ZnPc-PMMA7	688.5	359.0

Steady-state fluorescence spectra were performed both for ZnPc-Br and ZnPc-PMMA4 for the concentration of  $1.7 \times 10^{-5}$  M in DMF and the excitation wavelength was set to 630 nm for the Q band as seen in Figure 11. Calculated Stokes shift values were typical of Pc complexes. The fluorescence spectra of ZnPc-PMMA4 were similar.

As described in the literature,<sup>56</sup> Eq. (1), using the comparative method, was employed to find the quantum yields of the Pcs. The quantum yield of a compound in this method is determined by using a standard compound that has similar fluorescent properties with the compound tested. All the measurements of the standard and the compound must be carried out at identical environmental conditions along with same settings



**Figure 11.** Fluorescence emission spectra of ZnPc-Br and ZnPc-PMMA4.

of instruments.

$$F = (Std) \frac{F A_{Std} \eta^2}{F_{Std} A \eta_{Std}^2} \quad (1)$$

In Eq. (1),  $F$  is the value of the area under the fluorescence curves of Pc compounds and  $F_{Std}$  is the value of the area under the fluorescence curve of the standard.  $A$  and  $A_{Std}$  are the absorbance values of the sample and standard at emission while  $\eta$  and  $\eta_{Std}$  are the refractive index values of solvents used for the sample and standard, respectively. Absorption and fluorescence emission spectral data are summarized in Table 5. ZnPc-1 was chosen ( $\Phi F = 0.23$ ) as a standard in dimethylformamide. Similar to zinc Pcs in the literature, the fluorescent quantum yield ( $\Phi F$ ) value for ZnPc-Br was found to 0.29. The fluorescence quantum yield of ZnPc-PMMA4 could not be calculated because there were not any references available for them.

**Table 5.** Absorption and fluorescence emission spectral data.

Compound	Q band $\lambda_{max}$ (nm)	Emission $\lambda_{Em}$ (nm)	Stokes shift (nm)	$\Phi F$	Reference
ZnPc-Br	687.5	696.0	8.5	0.290	
ZnPc-PMMA4	688.0	696.0	8.0	-	
ZnPc-1	677.0	687.0	10.0	0.230	. <sup>57</sup>

## 2.6. Transmittance properties

Transmittance properties of thin films prepared with Pc and polymer Zn-PMMA4 on a glass substrate were observed by UV-Vis spectrophotometer. Table 6 shows the data taken from transmittance spectra. It can be seen that the transmittances of pure PMMA and ZnPc-PMMA synthesized using Pc as an initiator are not very different, so we can say that using Pc as an initiator does not have a negative effect on the transmittance of the films. The transmittance results of Pcs indicate that they can be used as an optical filter between 300–400 nm and 600–700 nm.

## 2.7. Conclusions

In summary, ZnPc-Br, a new ATRP initiator having active bromine groups at the periphery, was synthesized and used to perform ATRP of MMA in the presence of Cu(I) bromide and PMDETA. The structures of all synthesized compounds were characterized using  $^1\text{H}$  NMR and FTIR spectral techniques. Electrochemical

**Table 6.** Transmittance spectral data of ZnPc-Br, ZnPc-PMMA4, Std. PMMA.

Sample	T% (visible region) <sup>a</sup>	T% (near-UV region) <sup>b</sup>
ZnPc-Br	93	88
ZnPc-PMMA4	90	90
Std. PMMA	92	93

<sup>a</sup> Visible region values were taken between 600 and 700 nm.

<sup>b</sup> Near-UV region values were taken between 300 and 400 nm.

studies were performed on Pc initiators and obtained polymers and the results were compatible with those of similar complexes reported in the literature. A narrow molecular weight distribution was observed with the synthesized ZnPc-PMMA. Controlled/living polymerization of MMA using ZnPc-Br as an initiator for ATRP showed a linear relationship for both  $\ln[M]_o/[M]_t$  vs. time and molecular weight vs. conversion. The DSC results have a good correlation with those of pure PMMA polymer. Introducing the PCs as a core structure into the polymer did not make any considerable change to the residue amount in the TGA analysis. UV-Vis analysis showed that ZnPc-PMMA had properties similar to Pcs; however, they began to lose their fluorescence properties with increasing molecular weight. Transmittance properties of the initiator and ZnPc-PMMA were examined and showed that there were no negative influences on transmittance when PMMA was synthesized using ZnPc-Br as an initiator. The design of Pc-containing polymeric materials is a novel alternative to create new functional materials with attractive physical properties exclusive of other conventional polymers.

### 3. Experimental

#### 3.1. Materials

The preparation of ZnPc-OH was performed according to a literature procedure.<sup>41</sup> 2-Bromopropionyl bromide (97%, Sigma Aldrich), triethylamine (TEA, 99%, Acros), 4-dimethylaminopyridine (DMAP, Fluka), dimethylformamide (DMF,  $\geq 99.5\%$ , Merck), sodium carbonate (Lachema), anisole ( $\geq 99\%$ , Acros), copper(I) bromide (98%, Sigma Aldrich), *N,N,N',N',N''*-pentamethyldiethylenetriamine (PMDETA, 97%, Aldrich), tetrahydrofuran (THF, 99.8%, J. T. Baker), and methyl alcohol ( $\geq 99\%$ , Sigma) were used as received.

An alumina column was employed just prior to use to remove the inhibitor contained in methyl methacrylate (MMA, 98%, Fluka). Before use, MMA was distilled in vacuo over calcium hydride.

#### 3.2. Characterization and analysis

A Thermo Scientific Nicolet IS Fourier transform spectrometer was used for acquiring FTIR analyses. The spectral resolution was  $4\text{ cm}^{-1}$ . Working in the range of  $4000\text{--}400\text{ cm}^{-1}$ , an average of 16 scans were recorded for each sample. <sup>1</sup>H NMR analyses were acquired at 500 MHz with a spectrometer of the Agilent VNMRs brand. DMSO-*d*<sub>6</sub> (deuterated dimethyl sulfoxide) and CDCl<sub>3</sub> (deuterated chloroform) were used as deuterated solvents. An Agilent pump, a refractive index detector, and three Agilent Zorbax PSM 1000S, 300S, 60S columns ( $6.2 \times 250\text{ mm}$ ,  $5\ \mu\text{m}$ ) to measure within the ranges of  $10^4$  to  $10^6$ ,  $3 \times 10^3$  to  $3 \times 10^5$ , and  $5 \times 10^2$  to  $10^4$ , respectively, were employed in the GPC analyses. With a flow rate of 0.5 mL/min at a temperature of 30 °C, our chosen eluent was THF. Molecular weights were calculated by referring to the PMMA standards. UV-Vis analyses were performed with a Shimadzu PharmaSpec UV 1700 UV-Vis spectrophotometer. Dimethylformamide was

used for blank solution. Mass spectra were measured on a Bruker Microflex LT using dithranol as the matrix. DSC, with an instrument of the TA DSC Q10 brand, in a flowing nitrogen atmosphere, was started from 30 °C at a scanning rate of 10 °C/min. For TGA, a TA Q50 instrument was run under nitrogen atmosphere at a heating rate of 20 °C per min, and the temperature was raised from room temperature to 750 °C. The sample weights used in this study were between 6 and 10 mg. As reference material for calibration, indium was used.

Florescence spectroscopy analyses were performed with a Varian Clay Eclipse fluorescence spectrophotometer. Excitation wavelength was 630 nm.

For cyclic voltammetry (CV) and square wave voltammetry (SWV), we used a Gamry Reference 600 potentiostat/galvanostat, utilizing a conventional three-electrode cell configuration at room temperature in DMF solutions. A glassy carbon electrode was employed as the working electrode, whose surface area was 0.071 cm<sup>2</sup>. As the counter electrode, platinum wire was used, and the reference electrode was a SCE. The scan rate was 25 mV/s. An Agilent 8453E UV-Vis spectrophotometer was employed to measure the transmittance of the films within the spectral range of 300–1100 nm.

### 3.3. Synthesis

#### 3.3.1. Synthesis of ZnPc-Br

A three-necked flask was charged with ZnPc-OH (0.27 g, 0.31 mmol), TEA (0.56 mL, 3.98 mmol), and DMAP (0.034 mmol, 0.0042 g), and DMF (25 mL) was added as a solvent. The reaction medium was cooled to 0 °C under nitrogen atmosphere. Then 2-bromopropionyl bromide (3.3 mmol, 0.35 mL) was added dropwise to the solution, and the mixture was stirred for 1 h at 0 °C and 96 h at room temperature. The reaction mixture was treated with dichloromethane and the mixture was washed with deionized water and 5% Na<sub>2</sub>CO<sub>3</sub> solution. After the evaporation of the solvent, the crude product was purified by using column chromatography with a chloroform/methanol mixture at 20/1 (v/v) as the eluent. ZnPc-Br exhibits a molecular-ion peak at  $m/z = 1421.604 [M+H]^+$  in the MALDI-TOF mass spectrum. Yield was 79%.

#### 3.3.2. Synthesis of ZnPc-PMMA

MMA (3.2 mL, 30 mmol), anisole (2 mL, 18.4 mmol), CuBr (0.015 g, 0.1 mmol), PMDETA (44 μL, 0.21 mmol), and initiator (ZnPc-Br; 0.02 g, 0.014 mmol) were mixed in a Schlenk tube. The Schlenk tube was sealed and cycled between vacuum and N<sub>2</sub> three times for removing the dissolved gases and then was put in an oil bath at 95 °C under continuous stirring. After polymerization was run for several hours (6, 12, 24, 48 h), the tube was cooled to room temperature, and the polymerization mixture was added to a sufficient amount of THF. A neutral alumina column was used to remove the copper complex from the THF solution and then excess THF was evaporated. The polymer was precipitated by pouring it into excess methanol; then vacuum filtration was employed to isolate it and finally it was dried under vacuum at room temperature. Gravimetric analysis was used for calculating the conversion.

#### 3.3.3. Film preparation

Thin films of the polymers were spin-coated by using an SCS P6700 spin-coater (1000 rpm for 30 s) onto a dried and clean glass substrate using the solutions prepared by adding 20 mg of the synthesized polymers in 5 mL of chloroform. Following spin-coating, the polymer films were kept in an oven for 2 h at 120 °C. With this procedure, the glass substrate was coated completely with the polymers.

## Acknowledgment

The authors wish to express their gratitude to the Scientific Research Projects Coordination Unit of İstanbul Technical University under Grant No. 38047, 2015.

## References

1. Löbber, G. In *Ullmann's Encyclopedia of Industrial Chemistry*; Wiley-VCH Verlag: Weinheim, Germany, 2000.
2. Guillaud, G.; Simon, J.; Germain, J. P. *Coord. Chem. Rev.* **1998**, *178-180*, 1433-1484.
3. Guldi, D. M.; Gouloumis, A.; Vazquez, P.; Torres, T. *Chem. Commun.* **2002**, 2056-2057.
4. Gursel, Y. H.; Senkal, B. F.; Kandaz, M.; Yakuphanoglu, F. *Polyhedron* **2009**, *28*, 1490-1496.
5. Durmus, M.; Yesilot, S.; Ahsen, V. *New J. Chem.* **2006**, *30*, 675-678.
6. Ishikawa, N.; Sugita, M.; Ishikawa, T.; Koshihara, S. Y.; Kaizu, Y. *J. Am. Chem. Soc.* **2003**, *125*, 8694-8695.
7. Chen, Y.; Hanack, M.; Blau, W. J.; Dini, D.; Liu, Y.; Lin, Y.; Bai, J. *J. Mater. Sci.* **2006**, *41*, 2169.
8. Hofman, J. W.; van Zeeland, F.; Turker, S.; Talsma, H.; Lambrechts, S. A.; Sakharov, D. V.; Hennink, W. E.; van Nostrum, C. F. *J. Med. Chem.* **2007**, *50*, 1485-1494.
9. Kolarova, H.; Nevrelova, P.; Bajgar, R.; Jirova, D.; Kejlova, K.; Strnad, M. *Toxicol In Vitro* **2007**, *21*, 249-253.
10. de Loos, F.; de la Torre, G.; Torres, T.; Cornelissen, J. J. L. M.; Rowan, A. E.; Nolte, R. J. M. *J. Phys. Org. Chem.* **2012**, *25*, 586-591.
11. McKeown, N. B. *J. Mater. Chem.* **2000**, *10*, 1979-1995.
12. de la Escosura, A.; Martínez-Díaz, M. V.; Torres, T.; Grubbs, R. H.; Guldi, D. M.; Neugebauer, H.; Winder, C.; Drees, M.; Sariciftci, N. S. *Chem. Asian J.* **2006**, *1*, 148-154.
13. Campo, B. J.; Duchateau, J.; Ganivet, C. R.; Ballesteros, B.; Gilot, J.; Wienk, M. M.; Oosterbaan, W. D.; Lutsen, L.; Cleij, T. J.; de la Torre, G. et al. *Dalton Trans.* **2011**, *40*, 3979-3988.
14. Dieter, W. *Macromol. Rapid Commun.* **2001**, *22*, 68-97.
15. Mineo, P.; Alicata, R.; Micali, N.; Villari, V.; Scamporrino, E. *J. Appl. Polym. Sci.* **2012**, *126*, 1359-1368.
16. Bilgin, A.; Yağcı, Ç.; Mendi, A.; Yıldız, U. *J. Appl. Polym. Sci.* **2008**, *110*, 2115-2126.
17. Zhao, L.; Yao, H.; Liu, Y.; Zhang, Y.; Jiang, Z. *J. Appl. Polym. Sci.* **2013**, *128*, 3405-3410.
18. Bilgin, A.; Yağcı, Ç. *Eur. Polym. J.* **2014**, *61*, 240-252.
19. Bilgin, A.; Yanmaz, D.; Yağcı, Ç. *Turk. J. Chem.* **2014**, *38*, 1135-1152.
20. Wöhrle, D. *Macromol. Rapid Commun.* **2001**, *22*, 68-97.
21. Li, Y.; Zhao, D.; Li, Y.; Liu, Y.; Duan, Q.; Kakuchi, T. *Dyes Pigm.* **2017**, *142*, 88-99.
22. Qiu, N.; Li, Y.; Han, S.; Satoh, T.; Kakuchi, T.; Duan, Q. *J. Appl. Polym. Sci.* **2014**, *131*, 40523.
23. Matyjaszewski, K.; Xia, J. *Chem. Rev.* **2001**, *101*, 2921-2990.
24. Aimi, J.; Wang, P. H.; Shih, C. C.; Huang, C. F.; Nakanishi, T.; Takeuchi, M.; Hsueh, H. Y.; Chen, W. C. *J. Mater. Chem. C* **2018**, *6*, 2724-2732.
25. Moad, G.; Rizzardo, E.; Thang, S. H. *Aust. J. Chem.* **2009**, *62*, 1402-1472.
26. Guillaneuf, Y.; Gigmès, D.; Marque, S. R. A.; Astolfi, P.; Greci, L.; Tordo, P.; Bertin, D. *Macromolecules* **2007**, *40*, 3108-3114.
27. Gao, Z.; Tao, X.; Cui, Y.; Satoh, T.; Kakuchi, T.; Duan, Q. *Polym. Chem.* **2011**, *2*, 2590-2596.
28. Zhang, J.; Wang, L.; Li, C.; Li, Y.; Liu, J.; Tu, Y.; Zhang, W.; Zhou, N.; Zhu, X. *J. Polym. Sci. A Polym. Chem.* **2014**, *52*, 691-698.
29. Kimura, M.; Ueki, H.; Ohta, K.; Hanabusa, K.; Shirai, H.; Kobayashi, N. *Chem Eur. J.* **2004**, *10*, 4954-4959.

30. Şen, B. N.; Mert, H.; Dinçer, H.; Koca, A. *Dyes Pigm.* **2014**, *100*, 1-10.
31. Heinrich, C. D.; Kostakoglu, S. T.; Thelakkat, M. *J. Mater. Chem. C* **2017**, *5*, 6259-6268.
32. Sütçüler, Y. A.; Sevim, A. M.; Çanak, T. Ç.; Serhatlı, İ. E.; Gül, A. *Dyes Pigm.* **2017**, *144*, 58-68.
33. Ganicz, T.; Makowski, T.; Stanczyk, W. A.; Tracz, A. *eXPRESS Polym. Lett.* **2012**, *6*, 373-382.
34. Dumoulin, F.; Durmuş, M.; Ahsen, V.; Nyokong, T. *Coord. Chem. Rev.* **2010**, *254*, 2792-2847.
35. Kaya, E. N.; Tuncel, S.; Basova, T. V.; Banimuslem, H.; Hassan, A.; Gürek, A. G.; Ahsen, V.; Durmuş, M. *Sens. Actuators B* **2014**, *199*, 277-283.
36. Kadem, B.; Göksel, M.; Şenocak, A.; Demirbağ, E.; Atilla, D.; Durmuş, M.; Basova, T.; Shanmugasundaram, K.; Hassan, A. *Polyhedron* **2016**, *110*, 37-45.
37. McKeown, N. B.; Painter, J. *J. Mater. Chem.* **1994**, *4*, 1153-1156.
38. Clarkson, G. J.; Hassan, B. M.; Maloney, D. R.; McKeown, N. B. *Macromolecules* **1996**, *29*, 1854-1856.
39. Kimura, M.; Narikawa, H.; Ohta, K.; Hanabusa, K.; Shirai, H.; Kobayashi, N. *Chem. Mater.* **2002**, *14*, 2711-2717.
40. Junko, A.; Chen-Tsyr, L.; Hung-Chin, W.; Chih-Feng, H.; Takashi, N.; Masayuki, T.; Wen-Chang, C. *Adv. Electron. Mater.* **2016**, *2*, 1500300.
41. Özçeşmeci, İ.; Okur, A. İ.; Gül, A. *Dyes Pigm.* **2007**, *75*, 761-765.
42. Wang, J. S.; Matyjaszewski, K. *Macromolecules* **1995**, *28*, 7572-7573.
43. Kamigaito, M.; Ando, T.; Sawamoto, M. *Chem. Rev.* **2001**, *101*, 3689-3746.
44. Patten, T. E.; Matyjaszewski, K. *Adv. Mater.* **1998**, *10*, 901-915.
45. Coessens, V.; Pintauer, T.; Matyjaszewski, K. *Prog. Polym. Sci.* **2001**, *26*, 337-377.
46. Patten, T. E.; Matyjaszewski, K. *Adv. Mater.* **1998**, *10*, 901-915.
47. Matyjaszewski, K. *J. Phys. Org. Chem.* **1995**, *8*, 197-207.
48. Fischer, H. *J. Polym. Sci. A Polym. Chem.* **1999**, *37*, 1885-1901.
49. Matyjaszewski, K. In *Controlled Radical Polymerization ACS Symposium Series 685*; American Chemical Society: Washington, DC, USA, 1998, pp. 2-30.
50. Shipp, D. A.; Matyjaszewski, K. *Macromolecules* **2000**, *33*, 1553-1559.
51. Duan, G.; Zhang, C.; Li, A.; Yang, X.; Lu, L.; Wang, X. *Nanoscale Res. Lett.* **2008**, *3*, 118.
52. Trombach, N.; Hild, O.; Schlettwein, D.; Wohrle, D. *J. Mater. Chem.* **2002**, *12*, 879-885.
53. Özkaya, A. R.; Hamuryudan, E.; Bayir, Z. A.; Bekaroğlu, Ö. *J. Porphyrins Phthalocyanines* **2000**, *4*, 689-697.
54. Karaoğlu, H. R. P.; Koca, A.; Koçak, M. B. *Synth. Met.* **2013**, *182*, 1-8.
55. Bohle, M.; Boyd, G. V.; Fischer, E.; Friedrich, K.; Grashey, R. *Houben-Weyl Methods of Organic Chemistry, Vol. E 9c, 4th Edition Supplement: Hetarenes III*; Thieme, London, 2014.
56. Özçeşmeci, İ. *Synth. Met.* **2013**, *176*, 128-133.
57. Scalise, I.; Durantini, E. N. *Biorg. Med. Chem.* **2005**, *13*, 3037-3045.